Received: 16 December 2019 | Accepted: 9 March 2020
DOI: 10.1002/hyp.13748

WILEY

SPECIAL ISSUE PAPER

Impact of flooded rice paddy on remotely sensed evapotranspiration in the Krishna River basin, India

Pardhasaradhi Teluguntla[1] | Dongryeol Ryu[1] | Biju George[1] | Jeffrey P. Walker[2]

[1]Department of Infrastructure Engineering, The University of Melbourne, Melbourne, Victoria, Australia

[2]Department of Civil Engineering, Monash University, Clayton, Victoria, Australia

Correspondence
Pardhasaradhi Teluguntla and Dongryeol Ryu, Department of Infrastructure Engineering, The University of Melbourne, Melbourne, Victoria, Australia.
Email: teluguntlasaradhi@gmail.com (P. T.) and dryu@unimelb.edu.au (D. R.)

Funding information
Australian Centre for International Agricultural Research, Grant/Award Number: ACIAR Project LWR-2007-113.

Abstract

Evapotranspiration (ET) is one of the major water exchange processes between the earth's surface and the atmosphere. ET is a combined process of evaporation from open water bodies, bare soil and plant surfaces, and transpiration from vegetation. Remote sensing-based ET models have been developed to estimate spatially distributed ET over large regions, however, many of them reportedly underestimate ET over semi-arid regions (Jamshidi et al., Journal of Hydrometeorology, 2019, 20, 947–964). In this work, we show that underestimation of ET can occur due to the open water evaporation from flooded rice paddies ignored in the existing ET models. To address the gap in ET estimation, we have developed a novel approach that accounts for the missing ET component over flooded rice paddies. Our method improved ET estimates by a modified Penman-Monteith algorithm that considered the fraction of open water evaporation from flooded rice paddies. Daily ET was calculated using ground based meteorological data and the MODIS satellite data over the Krishna River Basin. Seasonal and annual ET values over the Krishna Basin were compared with two different ET algorithms. ET estimates from these two models were also compared for different crop combinations. Results were validated with flux tower-based measurements from other studies. We have identified a 17 mm/year difference in average annual ET over the Krishna River Basin with this new ET algorithm. This is very critical in basin scale water balance analysis and water productivity studies.

KEYWORDS
evapotranspiration, flooded rice paddy, Krishna River basin, MODIS, remote sensing ET

1 | INTRODUCTION

Evapotranspiration (ET) is one of the major water exchange processes between the earth's surface to the atmosphere and it is the collective process of evaporation from bare soils, open water bodies, and plant surfaces and transpiration from vegetation (Li et al., 2009). ET is an important component of the hydrologic processes and plays a substantial role in regional and global climate through hydrological circulation. Reliable estimates of ET is required to solve several issues in agriculture, hydrology, water management, and climate studies (e.g., Allen, Pereira, Raes, & Smith, 1998; Gowda et al., 2008). ET is a key variable in estimation of crop coefficients and crop water requirements (Marek et al., 2006).

Precise estimation of ET is essential particularly in the water balance from the watershed to continental scales studies for scheduling and managing water resources. For example, precise estimation of ET for irrigated croplands is critical for water allocation, irrigation scheduling, assessing the water productivity, developing best management practices to reduce surface and groundwater deprivation, and assessing the impacts of agriculture management practices on water resources (Bastiaanssen et al., 2005).

There are many ET methods which can be categorized into two groups. (a) Conventional methods and (b) Satellite based ET algorithms. Conventional methods use surface meteorological data from ground stations. However, they are typically point measurements and consequently represent only a minor fraction of the landscape. To overcome shortcomings of conventional methods, satellite based ET algorithms can be used to calculate ET over large scales since remote sensing data measures a much larger area than that possible with surface measurements; satellite derived parameters often used to calculate ET include vegetation index and the land surface temperature (LST) (Allen, Tasumi, & Trezza, 2007a; Kustas et al., 2003; Tasumi, Allen, Trezza, & Wright, 2005).

Surface energy balance (SEB) are a group of satellite-based ET algorithms which use LST and are frequently used in water resources management. SEB models include: SEB system (Su, 2002), SEB algorithm for land (Bastiaanssen et al., 1998, b), simplified SEB (Senay, Budde, Verdin, & Melesse, 2007, Senay et al., 2013), and mapping ET at high resolution with internalized calibration (Allen et al., 2007a; Allen, Tasumi, & Trezza, 2007b; Tasumi et al., 2005). The major limitation of SEB models is that they require uniformly hot and cold pixels within the scene for reference. This necessitates medium to high resolution thermal infrared (TIR) data to provide reliable ET estimates in which the Landsat 7 60-m TIR band is the most common source. However, Landsat 7 only constantly collects imagery every 16 days. Furthermore, since TIR cannot accurately measure LST through clouds, the effective imagery collection in the tropics (largely cloudy) is limited to a few acquisitions over a crop season (Allen et al., 2007b; Kalma, McVicar, & McCabe, 2008). Due to the large pixel size of coarse-resolution imagery, it is difficult to find wet areas where latent heat flux can be assumed to be maximum and dry areas where latent heat flux can be assumed to be zero. However, due to frequent image acquisition, cloud free imagery is much more likely to be acquired than higher resolution imagery with less frequent revisit times. Given the above limitations, it may not be feasible to use SEB models to estimate sub-seasonal fluctuation of ET at large scales.

In recent decades, several studies developed ET models using remote sensing data from advanced very high resolution radiometer (AVHRR) and moderate resolution imaging spectroradiometer (MODIS) satellite images and eddy covariance flux towers to estimate spatially distributed ET over larger regions (Cleugh, Leuning, Mu, & Running, 2007; Ferguson, Sheffield, Wood, & Gao, 2010; Leuning, Zhang, Rajaud, Cleugh, & Tu, 2008; Mu, Zhao, & Running, 2011; Teluguntla, Ryu, George, & Walker, 2013; Vinukollu, Wood, Ferguson, & Fisher, 2011, Zhang et al., 2009). However, many of them reportedly underestimated ET over semi-arid regions (Jamshidi, Zandparsa, Pakparvar, & Niyogi, 2019). Many of these methods depend on leaf area index (LAI) and other empirically derived parameters integrated into the Penman-Monteith (PM) model. For example, Teluguntla et al. (2013) used spatially distributed ET estimates from a modified PM model with biome-specific conductance estimated using the normalized difference vegetation index (NDVI) to analyse water balance. However, Teluguntla et al. (2013) identified an important limitation of the model from the analysis of basin scale ET: the basin water balance resulted in a large overestimation of stream discharge, which indicated an underestimation of the basin-scale ET.

We hypothesize that ET underestimation is partly caused by the modified PM model that doesn't account for the unique cultivation practice of the paddy rice widespread in India. Unlike most other crop fields, the rice paddy maintains ponded surface state for the 55–60% of the whole growing period. The LAI-based parameterization of the canopy resistance employed in the modified PM model does not consider the influence of the ponded surface and consequently may result in reduced ET from the combined canopy and water surface, particularly in the semi-arid climate (Moratiel & Martínez-Cob, 2013). Consequently, it is necessary to improve the ET models relying on the biome-specific conductance parameterization to account for rice paddies or similar surface conditions.

Rice is a main calorie source for over 50% of the world's population. About 154 million ha of rice was harvested across the world in 2010, out of which about 40% was harvested in South Asia (Gumma, Nelson, Thenkabail, & Singh, 2011) and overall about 88% was harvested in Asia. The majority of the rice paddy area in South and Southeast Asia are flood irrigated (Mohanty, 2014; Mutert & Fairhurst, 2002), which means that the fraction of the open water evaporation is relatively high. Due to the higher fraction of ET from open water in flooded rice paddies, it is likely that the existing ET algorithms/models underestimate ET over the rice-dominant regions in Asia. This is especially important in South and Southeast Asia as this may add significant uncertainty to the regional-to-continental water budget and subsequent water management and planning. Thus, a deeper understanding of the uncertainty of ET estimates might help to better determine water availability for agriculture. This work aims to improve the modified PM algorithm (Teluguntla et al., 2013; Zhang, Kimball, Nemani, & Running, 2010) to account for the fraction of open water evaporation from flooded rice paddies. This can help water-resource managers and water allocation authorities make informed decisions to supply water in scarce or crisis situations.

This study estimates ET by combining MODIS imagery and ground-based meteorological data. The 8-day composites of 250 m NDVI derived from MOD09Q1 product are used for the period June 2000–May 2007. A new ET model is applied in the Krishna River Basin, India to estimate the basin-scale ET over this time period. We have gathered a good set of ground based daily meteorological data from three different sources for the study period. This paper describes the novel approach that was used for estimating the spatially distributed ET to account for the fraction of open water from flooded rice paddies and compared annual ET for different crop combinations.

2 | STUDY AREA AND DATASET

2.1 | Study area

Our current study conducted in the Krishna River Basin (Figure 1), which is one of the largest river basins of India in terms of drainage area. The study area is located in the southern part of India lying

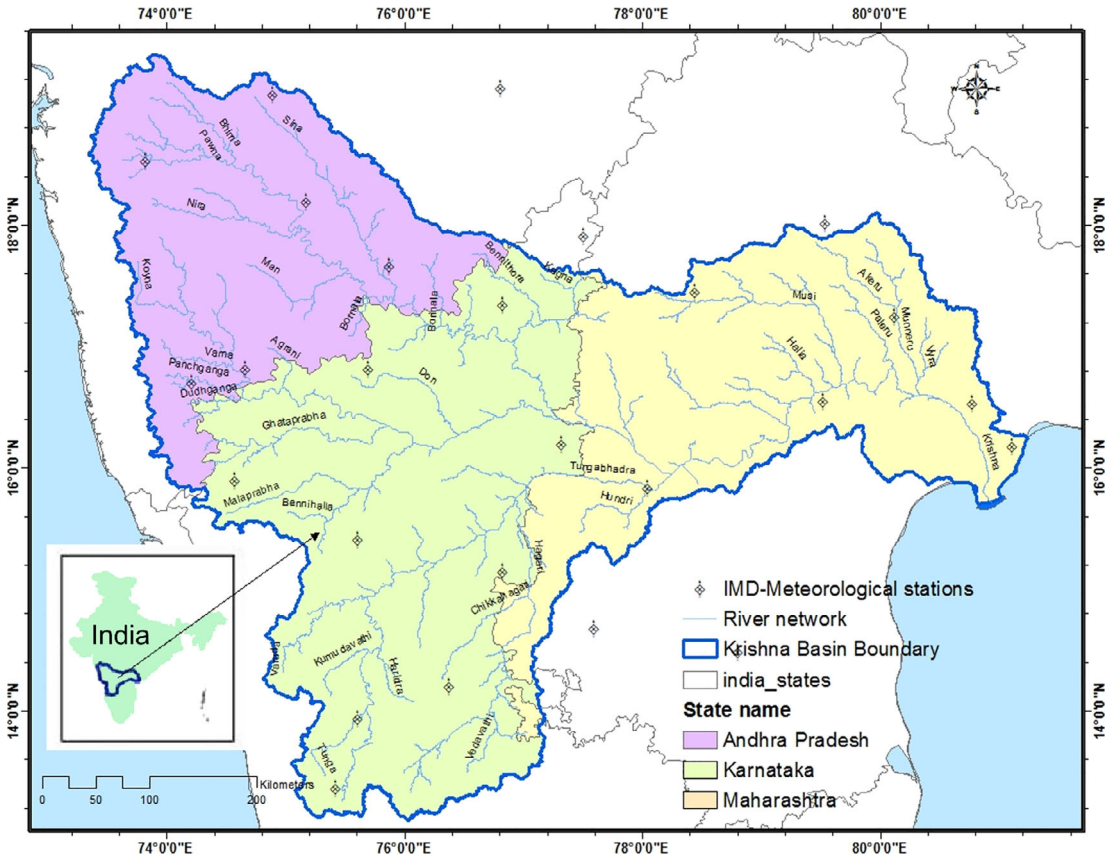

FIGURE 1 Location map of the study area with ground meteorological stations and river network generated using Shuttle Radar Topography Mission (SRTM) 90 m Digital Elevation Model (DEM)

between eastern longitudes 73°15′E and 81°15′E, and northern latitudes 13°05′N and 19°20′N. The geographical area covers four Sothern states including Maharashtra, Karnataka, Andhra Pradesh, and the newly formed Telangana State. Approximately about 265, 272 sq. km of total geographical area (Gumma et al., 2011). The river Krishna is an east flowing river originating in the Western Ghats that drains towards east and finally merge in the Bay of Bengal. The climate is primarily semi-arid along with some sub humid areas in the eastern region and some humid regions in the western region of the basin. Mean precipitation is about 800 mm per year (Teluguntla, Ryu, George, Walker, & Malano, 2015). Cropping occurs in two main seasons called kharif and rabi (Gumma, Thenkabail, Muralikrishna, et al., 2011). Also, there is some cropping during summer months (April and May), but it is not considered in this study.

Rice paddy is one of the main irrigated crops grown in the study area. Some farmers grow rice in kharif, some farmers grow in rabi (called single crop rice) or in both seasons (called double crop rice) depending on availability of water. Most of the rice crop is grown under flooded irrigation either by surface or ground water. There are some other irrigated crops also grown in the study area, which include commercial crops such as cotton, sugarcane, chilies, fodder grass, and pulses etc., (Teluguntla et al., 2015). Whereas dry-land crops such as millets, sorghum, oilseeds, legumes are grown in the rain-fed areas.

2.2 | Datasets and description

2.2.1 | Meteorological data

Remote sensing-based ET models primarily require climatological variables from ground stations and vegetation parameters from remote sensing products as inputs. We have acquired ground based meteorological data from three different sources for this study. The complete set of daily metrological data available from ground stations in the study area (Figure 1) was obtained from the Indian Metrological Department provided by the Government of India. In addition, we also obtained daily meteorological data from two other national and international research institutions for the study period.

2.2.2 | MODIS surface reflectance data

MODIS is an optical sensor with the Terra and Aqua satellites. MODIS scans the entire surface of the Earth twice a day, once per satellite, acquiring data in 36 spectral bands. The first seven bands of MODIS are designed for the study of land surfaces and vegetation. Of these, four bands including red, near infrared (NIR), blue and short-wave infrared (SWIR) (Table 1) capture the seasonal variations in vegetation vigour, surface water, and soil moisture that characterise key stages

TABLE 1 Specifications of the MODIS-Terra bands used for calculation of required indices for this study[a]

MODIS bands	Sub-division	Band width (nm)	Band center wavelength (nm)	Spatial resolution (m)	MODIS product
1	Red	620–670	648	250	MOD09Q1
2	NIR	841–876	858	250	MOD09Q1
3	Blue	459–479	470	500	MOD09A1
6	SWIR	1,628–1,652	1,640	500	MOD09A1

Note: We have used band 1, band 2, band 3 and band 6 in this study.
Abbreviations: MODIS, moderate resolution imaging spectroradiometer; NIR, near infrared; SWIR, short-wave infrared.
Source: http://modis-land.gsfc.nasa.gov.
[a]MODIS acquire data in 36 spectral bands, out of which the first 7 bands are specially designed for land studies.

of agriculture. The MODIS 8-day composites from the Terra satellite was used in this work. We have used the 250-m MOD09Q1 8-day product for red and NIR bands, the 500 m MOD09A1 8-day product for blue, and SWIR bands. The 8-day composites of MODIS products MOD09Q1 and MOD09A1 were downloaded from http://modis-land.gsfc.nasa.gov for the study period. We have resampled blue and SWIR bands to 250 m spatial resolution since red and NIR band data are available in 250 m spatial resolution. As we have used 8-day composite products, we have 46 composites per year. We have calculated the following indices for every 8-day period using surface reflectance values from the red, NIR, blue, and SWIR bands.

$$\mathrm{NDVI} = \frac{\mathrm{NIR} - \mathrm{RED}}{\mathrm{NIR} + \mathrm{RED}}, \tag{1}$$

$$\mathrm{EVI} = 2.5\frac{\mathrm{NIR} - \mathrm{RED}}{\mathrm{NIR} + 6{*}\mathrm{RED} - 7.5{*}\mathrm{BLUE} + 1}, \tag{2}$$

$$\mathrm{LSWI} = \frac{\mathrm{NIR} - \mathrm{SWIR}}{\mathrm{NIR} + \mathrm{SWIR}}. \tag{3}$$

2.2.3 | Land use land cover map

Land use and land cover (LULC) maps are one important input for Modified PM based ET estimates. We have used time series of MODIS 250 m, 8-day composite data for the year 2000–01 and applied the methodology developed by Thenkabail, Gangadhararao, Biggs, et al. (2007), Biggs et al. (2006), and Gumma, Thenkabail, Muralikrishna, et al. (2011); Gumma, Thenkabail, and Nelson (2011) to produce LULC maps for this study. The LULC map composed of 12 different land classes was derived from the MODIS 250 m, 8-day maximum value composites data and used it in ET retrieval.

2.2.4 | Flooded rice paddy map

A flooded rice paddy map is a key input for the new ET algorithm development in this study. We have adopted methodology established by Teluguntla et al. (2015) to map flooded rice paddies in our study area with MODIS 250 m 8-day composite time series data. With this we have produced seasonal flooded rice paddy maps for the study region from 2000–01 to 2006–07.

3 | METHODS

3.1 | Evapotranspiration algorithm

Prior to this study in the same study region, Teluguntla et al. (2013) used ET algorithm developed by Zhang et al. (2010) as a baseline to estimate ET by using local ground based meteorological data and global inventory modelling and mapping studies AVHRR NDVI data to improve ET estimates. But the algorithm fails in accounting for the evaporation fraction from open water covered by canopy. To address the gap in ET estimation, with this research, we have established a novel algorithm that accounts for the fraction of open water evaporation from flooded rice paddies.

3.2 | Weighted canopy method

For estimating ET from sparse canopy, Shuttleworth and Wallace (1985) developed an approach (SW) that separates ET into two components, soil evaporation and transpiration. Wessel and Rouse (1994) also developed a similar approach (WR) but accounted for evaporation from both soil and the water surface as well.

First. open water evaporation is estimated using Prestley and Taylor (PT) model (Priestley & Taylor, 1972) for water body pixels.

PT equation is used to calculate open water evaporation from

$$\lambda E_{\mathrm{openwater}} = a\frac{\Delta A}{\Delta + \gamma}, \tag{4}$$

$\lambda E_{\mathrm{openwater}}$ is the latent heat flux of open water, A is available energy, $\Delta = de_{\mathrm{sat}}/dT$ the slope of the curve relating saturated water vapour pressure (e_{sat}) to air temperature (T), $\gamma$is psychometric constant.

Now the available energy (A) for the non-flooded rice paddy pixels area is linearly partitioned into two energy components canopy (A_{canopy}) and soil surface (A_{soil}) using fractional vegetation cover (fvc) (Mu, Heinsch, Zhao, & Running, 2007) as follows

$$A_{\mathrm{canopy}} = A \times fvc, \tag{5}$$

$$A_{\mathrm{soil}} = A \times (1 - fvc). \tag{6}$$

For the flooded rice paddy pixels, on the other hand, the available energy (A) is linearly partitioned into A_{canopy} for canopy and A_{soil} for

soil before rice transplantation and 1 week after last irrigation. During irrigation period (after transplantation and end of irrigation), the available energy (A) is linearly partitioned into A_{canopy} for the canopy and $A_{\text{openwatere}}$ for open water using fractional vegetation cover. Soil surface can be assumed to be zero from transplantation season to last irrigation. Open water evaporation is assumed to be zero before transplantation and 2 weeks after last irrigation application for flooded rice paddy pixels.

$$A_{\text{openwater}} = A \times (1 - fvc) \tag{7}$$

So total energy (A) before transplantation of rice and 1 week after last irrigation is

$$A = A_{\text{canopy}} + A_{\text{soil}}. \tag{8}$$

Total energy (A) after transplantation of rice until last irrigation for flooded rice paddy pixels is

$$A = A_{\text{canopy}} + A_{\text{openwater}}. \tag{9}$$

The PM equation is used to calculate vegetation transpiration as

$$\lambda E_{\text{canopy}} = \frac{\Delta A_{\text{canopy}} + \rho C_p (e_{\text{sat}} - e) \times g_a}{\Delta + \gamma (1 + g_a / g_s)}, \tag{10}$$

the latent heat of vaporization, ρ (kg m^{-3}) the air density, $\Delta = de_{\text{sat}}/dT$ the slope of the curve relating saturated water vapour pressure e_{sat} to air temperature (T), $e_{\text{sat}} - e$ is the vapour pressure deficit (VPD), C_p (J kg^{-1} K^{-1}) the specific heat capacity of air, γ is psychometric constant, and g_a (ms^{-1}) the aerodynamic conductance, g_s a term identical to canopy conductance g_c.

Soil evaporation is calculated using equation from Teluguntla et al. (2013) and Zhang et al. (2010), which is a combination of a complementary relationship suggested by Bouchet (1963) and the adjusted PM equation. The soil evaporation equation is.

$$\lambda E_{\text{Soil}} = \frac{\Delta A_{\text{Soil}} + \rho C_p \text{VPD} g_a}{\Delta + \gamma \times (g_a / g_{\text{totc}})} \times \text{RH}^{(\text{VPD}/k)}, \tag{11}$$

where $\text{RH}^{(\text{VPD}/k)}$ a moisture constraint on soil evaporation, which is an index of soil water deficit based on the complementary relationship where surface moisture status is linked to the evaporative demand of the atmosphere. The theory was that the soil moisture is reflected in the adjacent atmospheric moisture and RH is the relative humidity (%), k (Pa) is a parameter to fit the complementary relationship and reflects the relative sensitivity to VPD. It is adjusted for different vegetation types.

g_a is sum of g_{rh} and g_{ch}, g_{rh} (m/s) is the conductance to the radioactive heat transfer, g_{ch} (m/s) is the conductance to the convective heat transfer under the boundary layer conditions (g_{bl}) and assigned g_{bl} and g_{ch} as biome-specific constants. The g_{tot} (m/s) is the total aerodynamic conductance to vapour transport and the combination of aerodynamic and surface conductance components. The g_{totc} (m/s) is the corrected value for g_{tot} from the standard conditions for temperature and pressure using the correction coefficient, and g_{tot} is adjusted by land cover types.

Open water evaporation for flooded paddy rice pixels is calculated using the following equation

$$\lambda E_{\text{openwater}} = a \frac{\Delta A_{\text{openwater}}}{\Delta + \gamma} \tag{12}$$

4 | RESULTS AND DISCUSSIONS

During the study period 2000–01 to 2006–07, actual ET estimated using MODIS 250-m data, and daily meteorological data was used with the modified PM equation in two separate schemes. The first one considered flooded rice paddies (denoted by Scheme 1 hereafter) and the other scheme without considering rice paddies (denoted by Scheme 2 hereafter). In Scheme 1, we calculated daily ET using a new model described in Section 3, which included vegetation transpiration, soil evaporation and fraction of open water evaporation from flooded rice paddies based on crop calendar. In Scheme 2, daily ET was estimated without considering flooded rice paddies (as defined in Teluguntla et al., 2013).

First, the hydrological year (June–May) of the study area was divided into two cropping seasons to calculate seasonal ET, namely kharif and rabi. Season 1 (kharif) had 195 days (June first to mid-December), which included some fallow period before planting the crop and after harvesting the crop. Season 2 (rabi) had 170 days (mid-December to May 31st) which included some fallow period before planting the crop and after harvesting the crop. Subsequently, daily ET was converted into seasonal ET for both kharif and rabi seasons. Consequently, annual ET was calculated for the hydrological year 2000–01 for the study area. Before estimation of ET, we had derived spatially distributed flooded rice paddy maps for the kharif and the rabi seasons separately using MODIS time series imagery data according to the algorithm developed by Teluguntla et al. (2015).

4.1 | Comparison between ET from two schemes over flooded rice paddy pixels and sensitivities of difference to kharif and rabi

For seasonal comparison of estimated ET, we have classified flooded rice paddy pixels into three categories including: (a) kharif season single crop rice, (b) rabi season single crop rice, and (c) both kharif and rabi seasons double crop rice. ET estimated using Scheme 1 over flooded rice paddy pixels during kharif season ranged between 700–745 mm/season with an average of 735 mm/season. Whereas ET estimated using Scheme 2 ranged between 400–460 mm/season with the average resulting in 440 mm/season. This showed that approximately 295 mm of ET was underestimated for the flooded rice paddy pixels during the kharif season using Scheme 2. Similarly, for the rabi

TABLE 2 Range and average ET of flooded rice paddy pixels estimated using two ET models (with and without considering fraction of open evaporation from flooded paddy pixels)

Category		ET includes open water evaporation from flooded rice paddy (new ET model)	ET without including open water evaporation from flooded rice paddy (old ET model)	Difference
Kharif rice (single crop rice)	Range (mm)	700–745	400–460	285–300
	Average (mm)	735	440	295
Rabi rice (single crop rice)	Range (mm)	560–635	320–380	240–255
	Average (mm)	590	340	250
Kharif + rabi rice (double crop rice)	Range(mm)	1,270–1,345	700–840	500–570
	Average (mm)	1,325	780	545

Abbreviation: ET, evapotranspiration.

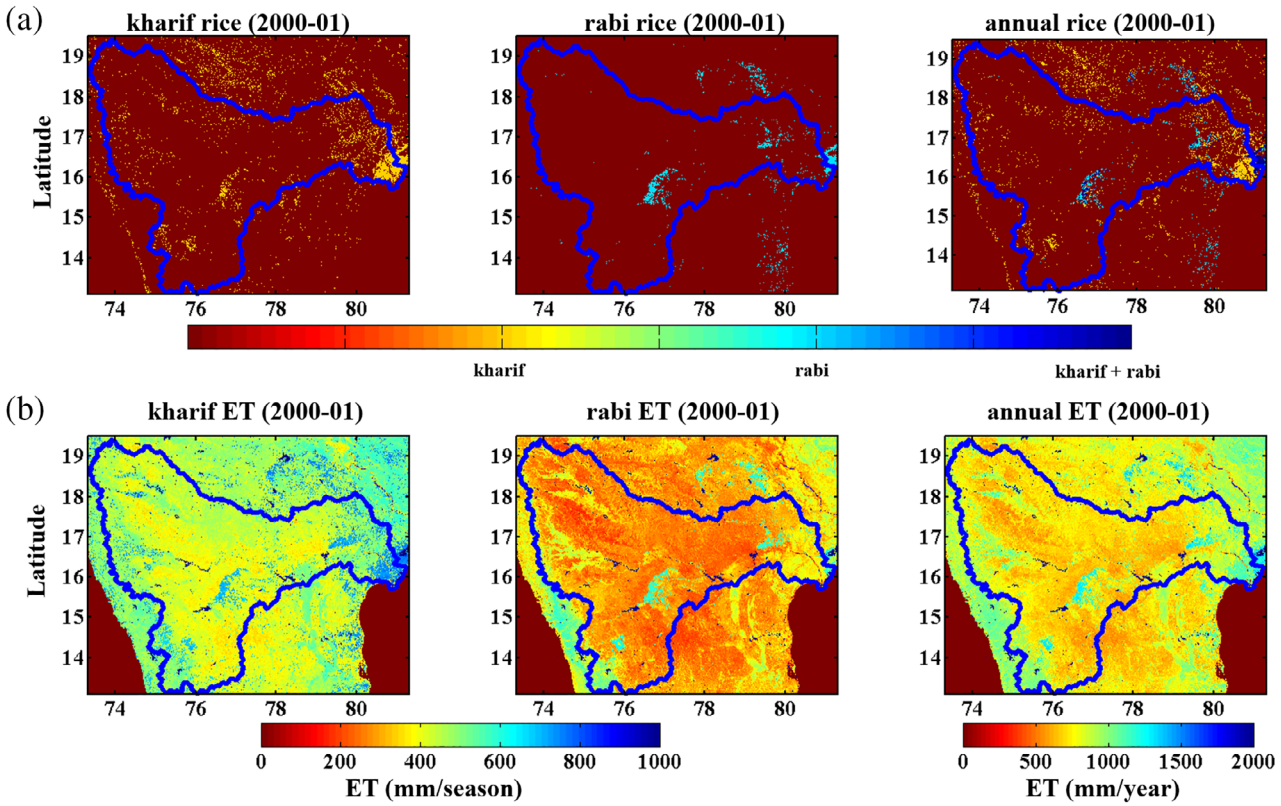

FIGURE 2 (a) Season wise rice paddy maps for the year 2000–01 derived using Teluguntla et al., 2015 (upper panel). (b) Season wise evapotranspiration (ET) maps for the year 2000–01 derived using new ET model by considering flooded rice paddies (lower panel)

season, Scheme 1 ET ranged from 565–635 mm/season with an average of 590 mm/season, and Scheme 2 ET ranged from 320–380 mm/season with an average of 340 mm/season. This showed that approximately 250 mm/season of ET was under-estimated for the flooded rice paddy pixels during the rabi season using Scheme 2.

For double crop rice pixels, Scheme 1 ET ranged between 1,270–1,345 mm/year with a mean of 1,325 mm/year. Whereas Scheme 2 ET ranged from 700–840 mm/season with a mean of 780 mm/season. This showed that approximately 545 mm/year ET was under-estimated for double crop rice area using the Scheme 2 ET model.

4.2 | Validation of ET from field studies

This study relied on literature for field ET validation; no field level ET measurements were directly made due to lack of field equipment. Based on available literature, ET estimated for flooded rice paddy pixels using Scheme 1 were compared with field level actual ET (ET*a*) measured/observed using flux tower studies by Alberto et al., 2011. Observed ET for the wet season (~kharif season) rice was 800 mm, which was measured for 211 days that included some fallow period; and dry season (~rabi season) rice ET was 592 mm for 155 days that also included some fallow period. The total ET observed for double

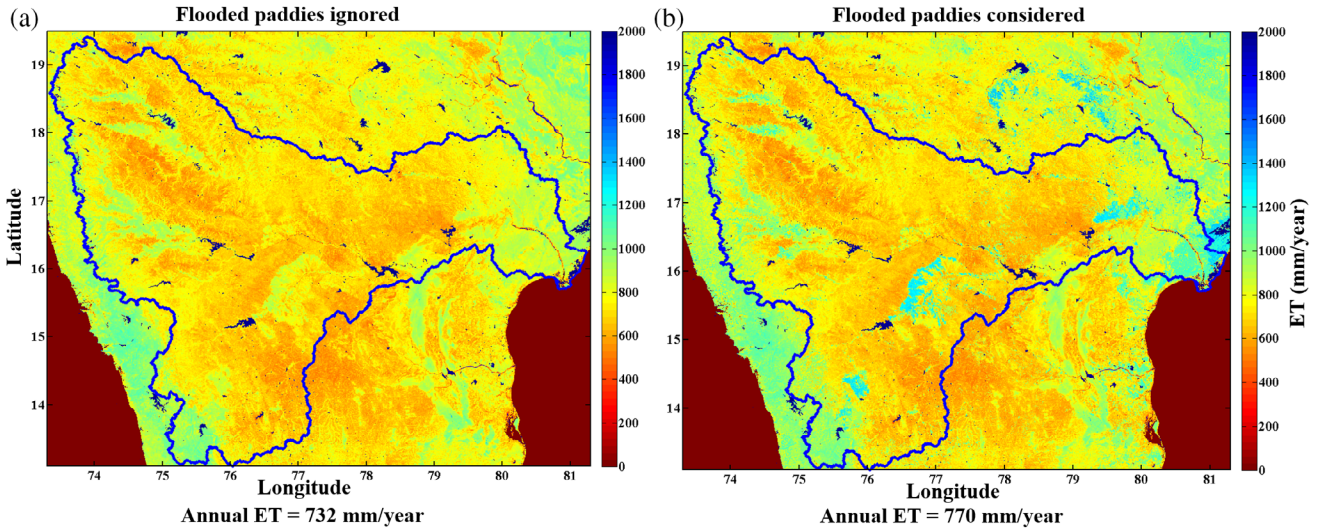

FIGURE 3 Comparison of spatially distributed annual evapotranspiration (ET) maps of Krishna River Basin for the year 2000–01. (a) ET Map with flooded paddies ignored (left panel, b) ET Map with flooded paddies considered (right panel)

crop rice was 1,392 mm for 365 days. Annual ET estimated (double crop rice ET) from the current study was 1,325 mm/year (Table 2) which is very close to the observed ET values from field studies. Season wise ET estimates are also very close to the observed values.

4.3 | Impact of including flooded-rice paddy-specific scheme on the basin-scale ET estimates

First, spatially distributed flooded rice paddy maps for kharif and rabi seasons were derived separately from MODIS imagery according to the procedure developed by Teluguntla et al., 2015. Figure 2a shows spatially distributed flooded rice paddy maps for kharif, rabi and annual (kharif + rabi) respectively for the growing season of 2000–01. Figure 2b shows spatially distributed ET maps for kharif, rabi and annual (kharif + rabi) respectively, which considered open water evaporation from flooded rice paddies for the year 2000–01. ET estimated using scheme1 was 463 mm for kharif season, 307 mm for rabi season and 770 mm/year for the year of 2000–01. Scheme 1 annual ET was 38 mm/year higher than ET estimated using Scheme 2, which was 732 mm/year. Annual ET comparisons from both schemes are shown in Figure 3.

Similarly, seasonal ET comparisons between the two schemes are shown in Figures 4 and 5. The maximum difference was observed in the kharif season, which was about a 31 mm difference when compared to basin scale ET, while an 8 mm difference was observed in the rabi season. During the kharif season, scheme1 ET showed 463 mm/season and Scheme 2 ET showed 432 mm/season (Figure 4). During the rabi season, scheme1 ET was estimated at 307 mm/season, while Scheme 2 ET was estimated at 299 mm/season (Figure 5). This resulted in that the flooded rice paddy area during the kharif season was higher than the rabi season. This implies that the estimated ET of flooded rice paddies was higher during the kharif season. In fact, there are huge amounts of fields cultivated with flooded rice paddies during the kharif season especially in the downstream section of the basin. Consequently, there is a large variation in estimated ET between the two ET schemes over flooded rice paddy pixels.

To compare ET between the two models, we have calculated basin scale daily ET using two schemes for the hydrological years 2000–01 to 2006–07, shown as annual ET in Table 3. This analysis found that there was a 17 mm/year difference in average annual ET between the two models, which is 2.36% of basin ET. The maximum difference between the two schemes was observed in 2000–01, which was 38 mm/year (5.19% of Basin ET) and the minimum difference was observed in 2003–04, which was 7 mm/year (1.01% of Basin ET). This difference is due to fluctuations in annual rainfall in the study area. The 2000–01 hydrological year was relatively wet year (Gumma, Thenkabail, Muralikrishna, et al., 2011) in the Krishna River Basin and year 2003–04 was the worst drought year in the basin during our study period (Teluguntla et al., 2015). Rice cropped area was high during the year 2000–01, due to surplus water supply for the rice crop. Rice cropped area significantly dropped during the year 2003–04 due to a water deficit in the basin. District wise agricultural statistics from Department of Agriculture also found a significant difference in rice cropped area between the above 2 years (Teluguntla et al., 2015).

5 | SUMMARY AND CONCLUSIONS

This study has shown that underestimation of ET can occur due to the open water evaporation from flooded rice paddies ignored in existing ET models. To address the gap in ET estimation, we have developed a novel approach that accounts for the missing ET component over flooded rice paddies. Our method improved ET estimates by a modified PM algorithm that considered the fraction of open water

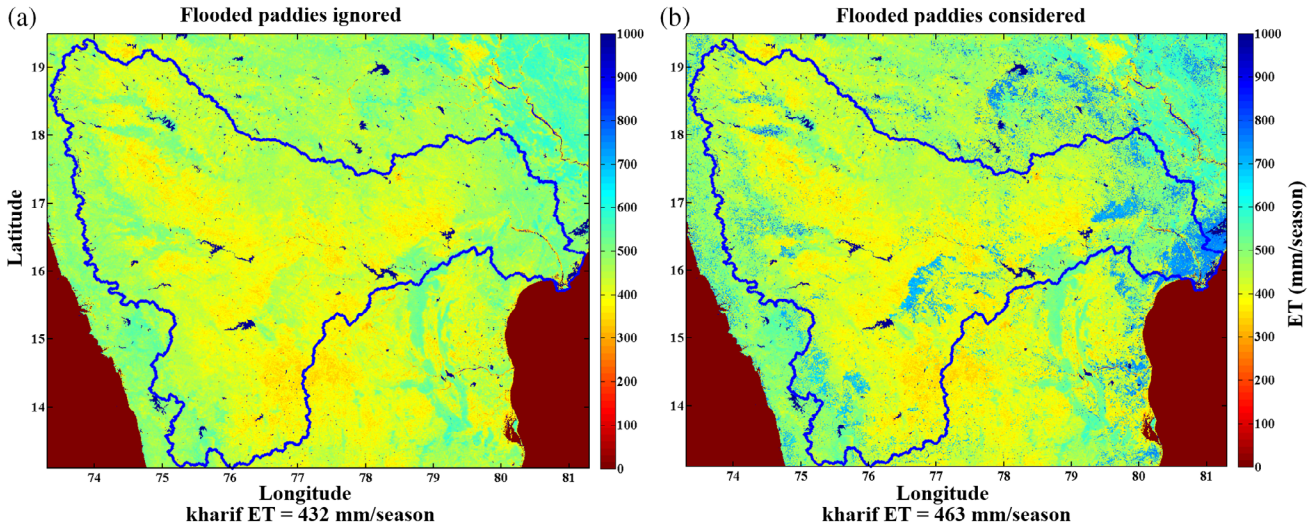

FIGURE 4 Comparison of spatially distributed evapotranspiration (ET) maps of Krishna River Basin during 2000–01 kharif season. (a) ET Map with flooded paddies ignored (left panel), (b) ET Map with flooded paddies considered (right panel)

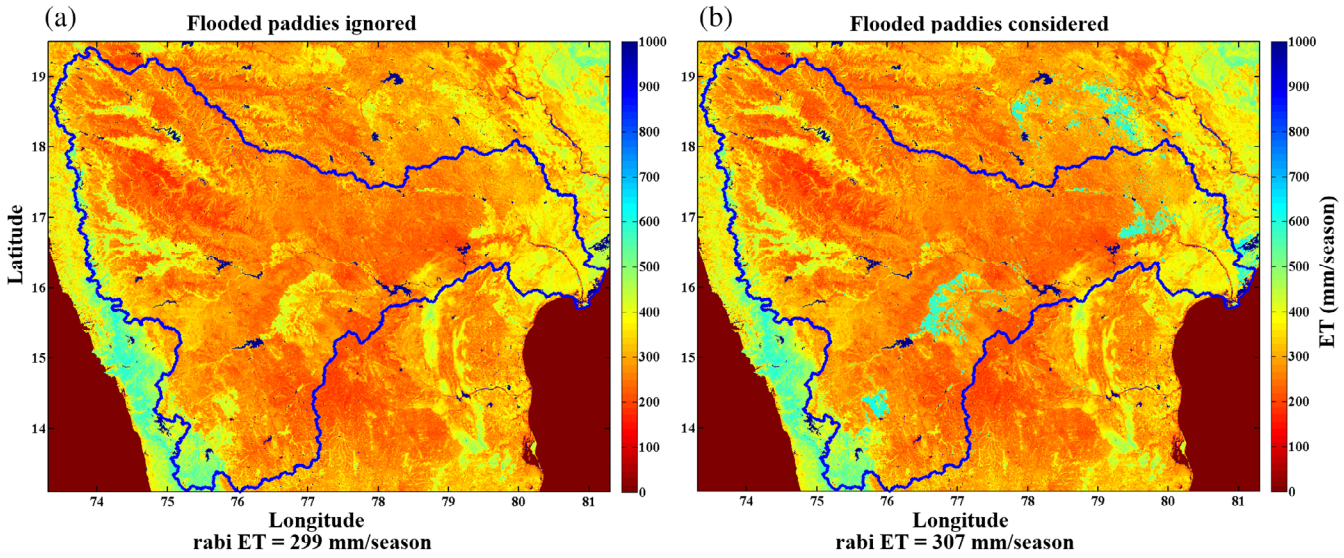

FIGURE 5 Comparison of spatially distributed evapotranspiration (ET) maps of Krishna River Basin during 2000–01 rabi season. (a) ET Map with flooded paddies ignored (left panel), (b) ET Map with flooded paddies considered (right panel)

TABLE 3 Comparison of annual ET estimated from two models (2000–01 to 2006–07)

Year	ET includes open water evaporation from flooded rice paddy Scheme 1 (mm/year)	ET without including open water evaporation from flooded rice paddy Scheme 2 (mm/year)	ET difference between the two models (mm/year)	Difference in ET(%)
2000–01	770	732	38	5.19
2001–02	738	725	13	1.79
2002–03	713	704	8	1.15
2003–04	709	702	7	1.01
2004–05	769	755	14	1.87
2005–06	768	745	23	3.09
2006–07	800	781	19	2.41
Average change in annual ET with new ET model (mm/year)			**17**	**2.36%**

Abbreviation: ET, evapotranspiration.

evaporation from flooded rice paddies. ET was calculated using the MODIS imagery and daily local meteorological data over the Krishna River Basin. Daily time series of ET maps were prepared using two ET models. Seasonal and annual ET over the Krishna River Basin was compared with two different schemes of ET algorithms. ET was also compared for different crop combinations. Results were validated with flux tower-based measurements from other studies. We have identified a 17 mm/year difference in average annual ET over the Krishna River Basin with a new ET algorithm. This is very critical in basin scale water balance analysis and water productivity studies in semi-arid regions. Although we applied this novel approach in the Krishna River Basin, the methodology developed here is not geographically limited to this study region. It can be applied in any other catchments with similar climatic conditions across the globe. This approach can be extended to larger regions such as sub-continental to continental scales if the required meteorological and land cover data are available. This study has shown that a robust ET estimate can be derived for flooded rice paddies; this methodology should be replicated in other rice paddy growing areas for further validation.

ACKNOWLEDGEMENTS

The authors would like to thank two anonymous reviewers and associate editor of HYP journal for providing constructive comments for the improvement of the manuscript. The research is funded by the ACIAR under the John Allwright Fellowship and the ACIAR Project LWR-2007-113. The authors would like to thank the International Water Management Institute (IWMI), International Crops Research Institute for Semi-Arid and Tropics (ICRISAT), Central Research Institute for Dry land Agriculture (CRIDA), the Indian Meteorological Department (IMD), and the Indian Institute of Tropical Meteorology (IITM) for providing daily ground meteorological and other ancillary data.

DATA AVAILABILITY STATEMENT

The data generated for this study is available from the corresponding author upon realistic request.

ORCID

Pardhasaradhi Teluguntla https://orcid.org/0000-0001-8060-9841

REFERENCES

Alberto, M. C. R., Wassmann, R., Hirano, T., Miyata, A., Hatano, R., Kumar, A., … Amante, M. (2011). Comparisons of energy balance and evapotranspiration between flooded and aerobic rice fields in The Philippines. *Agricultural Water Management*, *98*(9), 1417–1430.

Allen, R. G., Pereira, L. A., Raes, D., & Smith, M. (1998). *Crop evapotranspiration guidelines for computing crop water requirements. FAO irrigation and drainage Paper-56*. Rome: FAO.

Allen, R. G., Tasumi, M., & Trezza, R. (2007a). Satellite-based energy balance for mapping evapotranspiration with internalized calibration (METRIC) model. *Journal of Irrigation and Drainage Engineering*, *133*, 380–394.

Allen, R. G., Tasumi, M., & Trezza, R. (2007b). Satellite-based energy balance for mapping evapotranspiration with internalized calibration (METRIC) applications. *Journal of Irrigation and Drainage Engineering*, *133*, 395–406.

Bastiaanssen, W. G. M., Menenti, M., Feddes, R. A., & Holtslag, A. A. M. (1998). A remote sensing surface energy balance algorithm for land (SEBAL): Part I formulation. *Journal of Hydrology*, *213*, 198–212.

Bastiaanssen, W. G. M., Noordman, E. J. M., Pelgrum, H., Davids, G., Thoreson, B. P., & Allen, R. G. (2005). SEBAL model with remotely sensed data to improve water-resources management under actual field conditions. *Journal of Irrigation and Drainage Engineering*, *131*(1), 85–93.

Bastiaanssen, W. G. M., Pelgrum, H., Wang, J., Ma, Y., Moreno, J. F., Roerink, G. J., & van der Wal, T. (1998). A remote sensing surface energy balance algorithm for land (SEBAL): Part II validation. *International Journal of Hydrology*, *213*, 213–229.

Biggs, T., Thenkabail, P., Gumma, M., Scott, C., Parthasaradhi, G., & Turral, H. (2006). Irrigated area mapping in heterogeneous landscapes with MODIS time series, ground truth and census data, Krishna Basin, India. *International Journal of Remote Sensing*, *27*(19), 4245–4266.

Bouchet, R. J. (1963). Evapotranspiration réelle evapotranspiration potentielle, signification climatique. Paper presented at: Proceedings of Berkeley California Symposium. IAHS 62, pp.132–142.

Cleugh, H. A., Leuning, R., Mu, Q., & Running, S. W. (2007). Regional evaporation estimates from flux tower and MODIS satellite data. *Remote Sensing of Environment*, *106*, 285–304.

Ferguson, C. R., Sheffield, J., Wood, E. F., & Gao, H. (2010). Quantifying uncertainty in a remote sensing-based estimate of evapotranspiration over continental USA. *International Journal of Remote Sensing*, *31*, 3821–3865.

Gowda, P. H., Chavez, J. L., Colaizzi, P. D., Evett, S. R., Howell, T. A., & Tolk, J. A. (2008). ET mapping for agricultural water management: present status and challenges. *Irrigation science*, *26*(3), 223–237.

Gumma, M. K., Nelson, A., Thenkabail, P. S., & Singh, A. N. (2011). Mapping rice areas of South Asia using MODIS multitemporal data. *Journal of Applied Remote Sensing*, *5*(1), 053547.

Gumma, M. K., Thenkabail, P. S., Muralikrishna, I. V., Velpuri, M. N., Gangadhararao, P. T., Dheeravath, V., … Gaur, A. (2011). Changes in agricultural cropland areas between a water-surplus year and a water-deficit year impacting food security, determined using MODIS 250 m time-series data and spectral matching techniques, in the Krishna River basin (India). *International Journal of Remote Sensing*, *32*(12), 3495–3520.

Gumma, M. K., Thenkabail, P. S., & Nelson, A. (2011). Mapping irrigated areas using MODIS 250-meter time-series data: A study on Krishna River basin (India). *Water*, *3*(1), 113–131.

Jamshidi, S., Zand-parsa, S., Pakparvar, M., & Niyogi, D. (2019). Evaluation of evapotranspiration over a semiarid region using multiresolution data sources. *Journal of Hydrometeorology*, *20*(5), 947–964.

Kalma, J. D., McVicar, T. R., & McCabe, M. F. (2008). Estimating land surface evaporation: A review of methods using remotely sensed surface temperature data. *Surveys in Geophysics*, *29*(4-5), 421–469.

Kustas, W. P., Norman, J. M., Anderson, M. C., & French, A. N. (2003). Estimating sub pixel surface temperatures and energy fluxes from the vegetation index-radiometric temperature relationship. *Remote Sensing of Environment*, *85*, 429–440.

Leuning, R., Zhang, Y. Q., Rajaud, A., Cleugh, H., & Tu, K. (2008). A simple surface conductance model to estimate regional evaporation using MODIS leaf area index and the Penman-Monteith equation. *Water Resources Research.*, *44*, W10419.

Li, Z. L., Tang, R., Wan, Z., Bi, Y., Zhou, C., Tang, B., … Zhang, X. (2009). A review of current methodologies for regional evapotranspiration estimation from remotely sensed data. *Sensors*, *9*(5), 3801–3853.

Marek, T., Piccinni, G., Schneider, A., Howell, T., Jett, M., & Dusek, D. (2006). Weighing lysimeters for the determination of crop water requirements and crop coefficients. *Applied Engineering in Agriculture*, *22*(6), 851–856.

Mohanty S. 2014, IRRI. Rice Today Vol. 13, No. 2. Rice in South Asia. http://irri.org/rice-today/rice-in-south-asia

Moratiel, R., & Martínez-Cob, A. (2013). Evapotranspiration and crop coefficients of rice (*Oryza sativa* L.) under sprinkler irrigation in a semiarid climate determined by the surface renewal method. *Irrigation Science*, *31*(3), 411–422.

Mu, Q., Heinsch, F. A., Zhao, M., & Running, S. W. (2007). Development of a global evapotranspiration algorithm based on MODIS and global meteorology data. *Remote Sensing of Environment*, *111*, 519–536.

Mu, Q., Zhao, M., & Running, S. W. (2011). Improvements to a MODIS global terrestrial evapotranspiration algorithm. *Remote Sensing of Environment*, *115*(8), 1781–1800.

Mutert, E., & Fairhurst, T. H. (2002). Developments in rice production in Southeast Asia. *Better Crops International*, *15*, 12–17.

Priestley, C. H. B., & Taylor, R. J. (1972). On the assessment of surface heat flux and evaporation using large scale parameters. *Monthly Weather Review*, *100*, 81–92.

Senay, G. B., Bohms, S., Singh, R. K., Gowda, P. H., Velpuri, N. M., Alemu, H., & Verdin, J. P. (2013). Operational evapotranspiration mapping using remote sensing andweather datasets:A new parameterization for the SSEB approach. *Journal of the American Water Resources Association*, *49*, 1–15. https://doi.org/10.1111/jawr.12057

Senay, G. B., Budde, M., Verdin, J. P., & Melesse, A. M. (2007). A coupled remote sensing and simplified surface energy balance approach to estimate actual evapotranspiration from irrigated fields. *Sensors*, *7*(6), 979–1000.

Shuttleworth, W. J., & Wallace, J. S. (1985). Evaporation from sparse crops-an energy combination theory. *Quarterly Journal of the Royal Meteorological Society*, *111*(469), 839–855.

Su, Z. (2002). The surface energy balance system (SEBS) for estimation of turbulent heat fluxes. *Hydrology Earth System Science*, *6*, 85–99.

Tasumi, M., Allen, R., Trezza, R. G., & Wright, J. L. (2005). Satellite-based energy balance to assess within-population variance of crop coefficient curves. *Journal of Irrigation and Drainage Engineering*, *13*, 94–109.

Teluguntla, P., Ryu, D., George, B., & Walker, J. P. (2013). Multidecadal trend of basin-scale evapotranspiration estimated using AVHRR data in the Krishna River basin, India. *Vadose Zone Journal*, *12*(3), 1–14.

Teluguntla, P., Ryu, D., George, B., Walker, J. P., & Malano, H. M. (2015). Mapping flooded Rice paddies using time series of MODIS imagery in the Krishna River basin, India. *Remote Sensing*, *7*(7), 8858–8882.

Thenkabail, P., GangadharaRao, P., Biggs, T., Krishna, M., & Turral, H. (2007). Spectral matching techniques to determine historical land-use/land-cover (LULC) and irrigated areas using time-series 0.1-degree AVHRR pathfinder datasets. *Photogrammetric Engineering & Remote Sensing*, *73*(10), 1029–1040.

Vinukollu, R. K., Wood, E. F., Ferguson, C. R., & Fisher, J. B. (2011). Global estimates of evapotranspiration for climate studies using multi-sensor remote sensing data: Evaluation of three process-based approaches. *Remote Sensing of Environment*, *115*, 801–823.

Wessel, D. A., & Rouse, W. R. (1994). Modelling evaporation from wetland tundra. *Boundary-Layer Meteorology*, *68*(1–2), 109–130.

Zhang, K., Kimball, J. S., Mu, Q., Jones, L. A., Goetz, S. J., & Running, S. W. (2009). Satellite based analysis of northern ET trends and associated changes in the regional water balance from 1983 to 2005. *Journal of Hydrology*, *379*, 92–110.

Zhang, K., Kimball, J. S., Nemani, R. R., & Running, S. W. (2010). A continuous satellite derived global record of land surface evapotranspiration from 1983 to 2006. *Water Resources Research*, *46*, W09522.

How to cite this article: Teluguntla P, Ryu D, George B, Walker JP. Impact of flooded rice paddy on remotely sensed evapotranspiration in the Krishna River basin, India. *Hydrological Processes*. 2020;1–10. https://doi.org/10.1002/hyp.13748